The 2009 IEEE/RSJ International Conference on
Intelligent Robots and Systems
October 11-15, 2009 St. Louis, USA

Reactive Planning for Olfactory-Based Mobile Robots

Shuo Pang and Fangming Zhu

Abstract— **Olfaction is a long distance sense, which is widely used by animals for foraging or reproductive activities. Olfaction plays a significant role in natural life of most animals. For some animals, olfactory cues are far more effective than visual or auditory cues in search for objects such as foods and nests. Although chemical sensing is far simpler than vision or hearing, navigation in a chemical diffusion field is still not well understood. Therefore, this powerful primary sense has rarely been used inside the robotics community. This paper presents an effective olfactory-based planning and search algorithms for using on mobile robots. Olfactory-based mobile robots use odors as a guide to navigate and track in the unknown environments. The planning algorithms are based on Bayesian inference theory and artificial potential field methods. Inputs to the algorithms include the measured flow and the detection or non-detection events that happened at the robot location. This methodology results in algorithms for predicting likelihood of source location versus position. The robot would then optimize a desired trajectory to navigate in the odor plume and locate the odor source location.**

I. INTRODUCTION

Olfaction is a long distance sense, which is widely used by animals for foraging or reproductive activities [10]: homing by Pacific salmon, homing by green sea turtles, foraging by Antartic procellariiform seabirds, foraging by lobsters, foraging by blue crabs, mating and foraging by insects. Olfaction plays a significant role in natural life of most animals. For some animals, olfactory cues are far more effective than visual or auditory cues in search for objects such as foods and nests. Although odor sensing is far simpler than vision or hearing, navigation in a chemical diffusion field is still not well understood [18]. Therefore, this powerful primary sense has rarely been used inside the robotics community. The paper considers the development of an effective olfactory-based planning and search algorithms for using on mobile robots or autonomous vehicles. The goal of the robot will be to locate the source of a chemical that is transported in a turbulent fluid flow.

Olfactory-based robots use odors as a guide to navigate and track in the unknown environments. At first thought this olfactory-based navigational capability seems fairly trivial, "as we have all experienced the intuitive reaction to turn to face up-wind when presented with the chemical signature of barbecue on the grill or a bread bakery" [9]. However, in a turbulent fluid flow environment, the turbulence of the fluid medium continuously stretches and twists the filaments of the odor plume. Even within the plume, the odor is distributed in a highly patchy manner that would cause an intermittent signal to be measure by a high bandwidth sensor. In addition, the temporal and spatial variations in the flow velocity cause the plume centerline to meander. Therefore, the olfactory-based navigation over long distances in real-world turbulent fluid fields is not trivial.

Robots with the olfactory-based navigation and search capabilities would be of great significance, both for civilian, military, and counter-terrorism applications, e.g., the detection of chemical leaks, locating unexploded mines and bombs, finding people in search and rescue operation, and locating biologically interesting phenomenon such as underwater hydrothermal vents. Additionally, robots with olfaction can also be useful for applications currently carried out by human with the collaboration of trained animals that have well developed sense of smell (e.g. dogs). The planning algorithm presented herein is relevant to the design of olfactory-based mobile robots, but the general idea of this algorithm could also be applied more broadly in the context of searching with sporadic cues and partial information.

A. Problem Overview

Olfactory-based planning is complicated by the nature of fluid flow and the resulting odor plume characteristics. An initial approach to designing the olfactory-based planning algorithms might attempt to calculate a concentration gradient with subsequent plume tracing based on gradient following. Gradient following based plume planning algorithms have been proposed for a few biological entities that operate in low Reynolds number environments [6]; however, gradient based algorithms are not feasible in environments with medium to high Reynolds numbers [11], [14], [22]. At low Reynolds numbers, the evolution of the odor distribution in the flow is dominated by molecular diffusion resulting in a odor concentration field that is reasonably well-defined by a continuous function with a peak near the source. At medium and high Reynolds numbers, the evolution of the odor distribution in the flow is turbulence dominated [27]. The flow contains eddying motions of a wide range of sizes that produce a patchy and intermittent distribution of the above threshold chemical [14], [24]. For an image of the plume, the gradient is time-varying, steep, and frequently in the wrong direction. Even so, such plume images are not available to the robots. Due to the rate of spatial and temporal variations in the flow

This work was supported in part by the Research Fund from National Key Laboratory of Autonomous Underwater Vehicle Technology and in part by Embry-Riddle Aeronautical University Internal Research Award

Shuo Pang is with the National Key Laboratory of Autonomous Underwater Vehicle Technology, Harbin Engineering University Harbin 150001, China, and with Faculty of Computer and Software Engineering, Embry-Riddle Aeronautical University, Daytona Beach, FL 32114, USA shuo.pang@erau.edu

Fangming Zhu is with the Department of Computer and Software Engineering, Embry-Riddle Aeronautical University, Daytona Beach, FL 32114, USA zhuf@erau.edu

and plume relative to the maneuvering limitations of existing robots, gradient computation and following is not practical.

If a dense array of sensors were distributed over an area through which a turbulent flow was advecting odor and the output of each sensor were averaged for a suitably long time (i.e., several minutes), then this average odor distribution would be Gaussian [29], [30]; however, the required dense spatial sampling and long time-averaging makes such an approach inefficient in a turbulence dominated environment [25]. It is known that the instantaneous odor distribution will be distinct from the time-averaged plume [14], [22]. The major differences include: the time-averaged plume is smooth and unimodal while the instantaneous plume is discontinuous and multi-modal; the time-averaged plume is time invariant (assuming ergodicity) while the instantaneous plume is time varying; instantaneous concentrations well-above the time-averaged concentration will be detected much more often than predicted by the Gaussian plume model. Such time-averaged plumes are useful for long-term exposure studies, but are not useful for studies of responses to instantaneously sensed odor [11], [22]. One of the reasons that olfaction is a useful long distance sense is the fact that instantaneous concentrations well above the time-average are available at significant distances from the source [13]. Turbulent diffusion results in filaments of high concentration odor at significant distances from the source, but also results in high intermittency [2], [14], [23]. Intermittency increases with downflow distance both due to the meander of the instantaneous plume caused by spatial and temporal variations in the flow and due to the increasing spread with distance of the filaments composing the instantaneous plume. High intermittency and large search areas motivate the need to acquire as much information as is possible from each odor detection event.

The challenge using olfaction on mobile robots is to design effective algorithms to trace the odor plume and determine the odor source location even though the odor source concentration is not know, the advection distance of the detected odor is unknown, and the flow varies with both location and time.

B. Literature Overview

Various studies have developed biomimetic robotic plume tracing algorithms based on olfactory sensing. The most commonly used olfactory-based planning algorithms is "chemotaxis", which was introduced by Berg and Brown [7], [8]. This strategy is based on the detection of a concentration difference between two chemical sensors and a steering mechanism toward the direction of higher concentration with a constant moving speed. Chemotaxis-based planning strategies yields smooth movement trajectories in the environment that the concentration is high enough to ensure its difference measured at two nearby locations is larger than typical fluctuations. Belanger and Willis [4], [5] presented plume tracing strategies inspired by moth behavior and analyze the performance in a "wind tunnel-type" computer simulation. The main goal of that study was to improve the understanding of moth interaction with an odor stimulus in a wind tunnel. Grasso et al. [13] evaluate biometric strategies and challenge theoretical assumptions of the strategies by implementing biometric strategies on their robot lobster. Li et al. [17], [16] develop, optimize, and evaluate a counter-turning strategy originally inspired by moth behavior. Vergassola et al. [31], [20] proposed a search algorithm, "infotaxis", based on information and coding theory. For infotaxis, information plays a role similar to concentration in chemotaxis. The infotaxis strategy locally maximizes the expected rate of information gain. Its efficiency was demonstrated using a computational model of odor plume propagation and experimental data on mixing flows. Infotactic trajectories feature zigzagging and casting paths similar to those observed in the flight of moths. Spears et al. [28], [32] developed a physics-based distributed chemical plume tracing algorithm. The algorithm uses a network of mobile sensing agents that sense the ambient fluid velocity and chemical concentration, and calculate derivatives based on formal principles from the field of fluid mechanics.

The fundamental aspects of these research efforts are sensing the chemical, sensing or estimating the fluid velocity, and generating a sequence of searcher speed and heading commands such that the motion is likely to locate the odor source. Typical maneuvers include: sprinting upflow upon detection, moving crosswind when not detecting, and manipulating the relative orientation of a multiple sensor array either to follow an estimated plume edge or to maintain the maximum mean reading near the central sensor. In each of these articles, the algorithms for generating speed and heading commands use only instantaneous (or filtered) sensor readings.

Most of previous research on olfactory-base robots focused primarily on the understanding of the methods used by biological entities to track plumes and the translation of those biological approaches to strategies for robots plume tracing. This paper builds on the previous results by augmenting such biologically inspired strategies with sensing, computational, and memory capabilities that may not be available to biological entities. For example, a biological entity may not be capable of remembering precisely where it has been, where it has previously detected odor, or what the recent flow history was. The biological entity is therefore unable to construct a 'map' by synthesis of odor detection and flow information over time and space. In contrast an engineered olfactory-based robot can employ precisely these kinds of inputs and approaches to improve the performance and robustness of strategies based solely on biologically inspired approaches. Such engineered and physics based approaches are presented herein.

II. Olfactory Based Planning

The basic idea of the olfactory-based planning problem is as follows. A mobile robot is constrained to maneuver within a search region. Within the region the robot should search for a specified chemical, for which a binary sensor is available. The mission starts with the robot searching

the region for the chemical plume. A binary sensor outputs 1 if the chemical concentration is above threshold or 0 if the chemical concentration is below threshold. If above threshold chemical is detected, the robot should trace the chemical plume to its source and accurately declare the source location. The assumptions made herein relative to the chemical and flow are that the chemical is a neutrally buoyant and passive scalar being advected by a turbulent flow. The robot is assumed to be capable of sensing position, and flow velocity.

In the spirit of information and coding theory, the olfactory-based planning problem might be thought of as a message sent by the source and transmitted to the robot with strong noise due to the random nature of odor propagation in the turbulent medium [31]. Therefore, our planning methodology is based on the Bayesian inference methods, which are commonly used decoding methods in the information and coding theory, to decode this message to estimate the unknown source location. Using the Bayesian methodology, the source-likelihood map is propagated through time and updated in response to both detection and nondetection events. Then, Artificial Potential Field (APF) method is used to plan optimal paths for the robot to locate the chemical source.

The basic idea of the approach is described as follows. The search area is subdivided into an (n $\times$ m) array of rectangular cells. An odor plume model in the turbulent flow was developed from the fact that the odor filament movement in the flow is a random walk superimposed on the drift downflow advection [3]. From this stochastic odor plume model, a source likelihood map was generated given the detection and non-detection events. Each cell in the search area holds a Likelihood Value (LV) that represents the confidence of the algorithm in the existence of the chemical source at that location. This representation was derived from the certainty grid concept that was originally developed by Moravec and Elfes [21]. Based on ideas from the literature of APF, each cell in the source likelihood map will generate a virtual attractive force on the robot. The sum of all virtual forces determines the subsequent direction and speed of travel. Once the robot moves to a new cell, the odor detection or non-detection information will be used to update the source likelihood map, so that a new potential field will be generated based on the updated source likelihood map. This APF based chemical plume tracing method is discussed further in Section II-C.

A. Odor Plume Model

One of the goal of olfactory-based navigation is to locate the odor source. We begin by developing an understanding of models for the distribution of odor plume in a turbulent flow. Unfortunately, it is very difficult (even impossible) to describe the instantaneous structure of odor plume in a turbulent flow. Alternatively, by developing probabilistic descriptions of the spatial and temporal evolution of the odor plume, we will be able to use the information sensed on the robot to estimate likely source locations.

For short-time-scale studies, various authors [3] model odor filament movement as a random walk (due to velocity fluctuation) superimposed on the downflow advection (due to mean velocity). Similar ideas were used in [12] to produce the plume simulation model used for debugging and initial evaluation of the chemical plume tracing algorithms. Based on such ideas, the position of a odor filament is modeled as

$$\dot{\mathbf{X}}(t) = \mathbf{U}(\mathbf{X}, t) + \mathbf{N}(t) \tag{1}$$

where $\mathbf{X} = (x, y)$ is the odor filament location, $\mathbf{U} = (u_x, u_y)$ is the mean flow velocity, and $\mathbf{N} = (n_x, n_y)$ is a random process with zero mean and (σ_x^2, σ_y^2) variance. The random process $\mathbf{N}$ will be assumed to be Gaussian (i.e., normally distributed).

Using the model of eqn. (1), it would be possible to derive forward algorithms that allow theoretical computation of the plume location if the source location is known.

B. Source Likelihood Map

While the previous section discussed the plume distribution map when the source location and flow are known, the problem we are trying to solve is actually the inverse problem: Given a flow record and a history of odor detection or non-detection events along the vehicle trajectory, where is the odor source likely to be [26]? This inverse problem is known to be difficult based only on concentration and velocity measurements from fixed and sparely located sensors.

In order to describe the statistics of the spatial evolution of the plume, we first consider a simple case: if the source released a odor filament at time t_l, what will the temporal and spatial distribution of this odor filament location be at any time $t_k > t_l$? Integrating eqn. (1), we can obtain,

$$\mathbf{X}(t_l, t_k) = \int_{t_l}^{t_k} \mathbf{U}(\mathbf{X}(\tau))d\tau + \int_{t_l}^{t_k} \mathbf{N}(\tau)d\tau + \mathbf{X}_s \tag{2}$$

where $\mathbf{X}(t_l, t_k)$ is the odor filament location at time t_k given that the odor filament was released from a source located at $\mathbf{X}_s = (x_s, y_s)$ at time t_l. The mean odor filament location at time t_k is $\bar{\mathbf{X}}(t_l, t_k) = \int_{t_l}^{t_k} \mathbf{U}(\mathbf{X}(\tau))d\tau + \mathbf{X}_s$. Define $\mathbf{W}(t_l, t_k) = \int_{t_l}^{t_k} \mathbf{N}(\tau)d\tau$ which is a Gaussian noise process with zero mean and variance $[(t_k - t_l)\sigma_x^2, (t_k - t_l)\sigma_y^2]$. Note, the variance of $\mathbf{W}(t_l, t_k)$ increases linearly with $(t_k - t_l)$. Therefore, the odor filament position $\mathbf{X}(t_l, t_k)$ distribution at time t_k is a Gaussian distribution with mean $\bar{\mathbf{X}}(t_l, t_k)$, and variance $[(t_k - t_l)\sigma_x^2, (t_k - t_l)\sigma_y^2]$.

Now if the robot detects this odor filament at location $\mathbf{X}_v$ in cell C_j at time t_k, what is the probability that the source is located in some cell C_i? Solving eqn. (2) for the possible source location yields

$$\mathbf{X}_s(t_l, t_k) = \mathbf{X}_v(t_k) - \int_{t_l}^{t_k} \mathbf{U}(\mathbf{X}(\tau))d\tau - \int_{t_l}^{t_k} \mathbf{N}(\tau)d\tau \tag{3}$$

where the vehicle location is in cell C_j and $\mathbf{X}_j$ is the center of cell C_j. We will use the center of each cell to represent the cell position throughout the whole paper. In fact, because the cell size is comparable to the size of the vehicle and small compared to the search area, when the vehicle is in

cell C_j, we will assume that $\mathbf{X}_v(t_k) = \mathbf{X}_j = (x_j, y_j)$. Since we only have the flow sensor measurements at discrete times $\{t_i\}_{i=0}^{k}$ and only at the vehicle location, $\int_{t_l}^{t_k} \mathbf{U}(\mathbf{X}(\tau)d\tau$ must be approximated as $\sum_{i=l}^{k-1} \mathbf{U}(\mathbf{X}_v(t_i))dt$. This approximation introduces additional error, since the flow vector does vary with location. Let $\mathbf{V}(t_l, t_k) = (v_x(t_l, t_k), v_y(t_l, t_k)) = \sum_{i=l}^{k-1} \mathbf{U}(\mathbf{X}_v(t_i))dt$, then eqn. (3) will become

$$\mathbf{X}_s(t_l, t_k) = \mathbf{X}_j - \mathbf{V}(t_l, t_k) - \mathbf{W}(t_l, t_k). \tag{4}$$

Note that, in eqn. (4) the quantity $\mathbf{X}_j - \mathbf{V}(t_l, t_k)$ is a computable variable (i.e. $\mathbf{X}_j$ is determined by the current vehicle location and $\mathbf{V}(t_l, t_k)$ can be computed from the flow velocity record) and the quantity $\mathbf{W}(t_l, t_k)$ is a zero mean Gaussian random variable. Therefore, $\mathbf{X}_s(t_l, t_k)$ is a Gaussian random variable with mean $\mathbf{X}_j - \mathbf{V}(t_l, t_k)$ and variance $(t_k - t_l)\sigma^2$.

Let P_i represent the probability of the source being at some location $\mathbf{X}_i$. Then P_i is computed as the probability of the $\mathbf{W}(t_l, t_k)$ that makes $\mathbf{X}_i$ a solution of eqn. (4).

The previous discussion considered the simple, but unrealistic case, where the source releases a single chemical filament. If chemical is continuously released from a stationary source during the time period $t \in [t_0, t_k)$, then there will be $F = N(t_{k-1} - t_0)$ chemical filaments in the air at time t_k. When the robot detects chemical in cell C_j at time t_k, it is not immediately possible to determine the time t_l when the chemical filament was released from the source. In fact, the time t_0 at which the chemical release starts is also not known, but is typically much earlier than the mission start time. The value of t_l affects how far the likelihood map will be integrated back through time. When compute P_i, we must account for all possible release times t_l. Therefore, the source likelihood vector π is computed as the summation of source probability vector P at different released time t_l.

$$\pi_i = \sum_{l=0}^{k} P_i(t_l) \tag{5}$$

If $k > 50$, we only account for up to 50 steps backward propagation. Therefore, π is always less than or equal to 50. By calculating the probability of source at the location $\mathbf{X}_i$ for $i \in [1, N]$, we will obtain a source likelihood vector π. The details of calculating source likelihood map could be found in [26].

C. Chemical Plume Tracing via Artificial Potential Field Methods

In the past decades, APF methods are rapidly gaining popularity in obstacle avoidance applications for mobile robots due to its mathematical simplicity and elegance. It is based on well-understood physical principles and has been successfully implemented on collections of robots. The idea of imaginary forces acting on a robot has been suggested by Andrews and Hogan [1], and Khatib [15]. In a potential field, the robot is attracted to the target while being repelled by obstacles in the workspace. The sum of all forces serves as the input force driving the robot to its desired destination while avoiding collisions with obstacles. Typically, the attractive potential fields and the repulsive potential fields are formulated separately, and the total potential field of the workspace is obtained by linear superposition of the two fields.

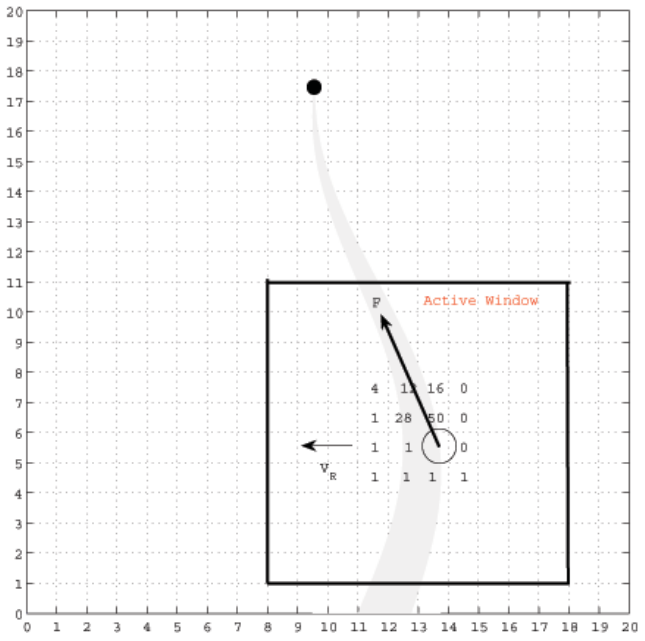

Fig. 1. The virtual force concept: Active cells generate attractive forces onto the robot. The numbers in each cell are the Likelihood Values (LV) of that cell. The black dot marks the source location. The circle indicates robot location. Robot is running from right to the left.

The potential field concept is applied to the olfactory-base navigation problems as shown in Fig. 1. It works as follows: As the vehicle moves, a window of $w \times w$ cells accompanies it, overlying a square region of $\mathbf{W}$. We call this region the "Active Window", and cells that momentarily belong to the active region are called "active cells". In Fig. 1 the size of the window is 10×10 cells, and the window is always centered about the robot's position. Each active cell generates a virtual attractive force on the vehicle. The magnitude of this force is proportional to LV (LV is proportional to the source likelihood vector π) and inversely proportional to the distance between the cell and the center of the vehicle. For Cell C_i the virtual force is

$$\mathbf{F}_i = \frac{LV_i}{d}\left(\frac{\mathbf{X_v} - \mathbf{X}_i}{d}\right), \tag{6}$$

where LV_i is the likelihood value of C_i, $d = \|\mathbf{X}_v - \mathbf{X}_i\|$ is the distance between cell C_i and the robot. All virtual forces add up to yield resultant virtual force $\mathbf{F}$,

$$\mathbf{F} = \sum_{i \in \mathbf{W}} \mathbf{F}_i. \tag{7}$$

The direction and magnitude of $\mathbf{F}$ are used as the reference for the robot's heading and speed command.

Fig. 1 shows a simple example of APF based chemical plume tracing. For illustrative purpose , the search area is a very small area, 20×20 cells. The chemical source is located in cell $C_{10,18}$, which is indicated by a black dot. The wind is mostly in "y-" direction with small variations between 240 and 300 degrees. The plume depicted in Fig. 1 is greatly simplified. Realistic plumes may meander, are intermittent or patchy distributions of chemical, and do not have a uniformly increasing width as a function of the distance from the chemical source. The robot starts the search from the cell $C_{20,6}$ and moves in the cross flow direction, i.e., the speed vector of robot is in "x-" direction. In the current snapshot, the robot is located in cell $C_{14,6}$, and it detects chemical in this cell. Based on this detect event and previous no detection events happened in cell $C_{15-20,6}$, a source likelihood map is calculated. Therefore, each cell in the active window will have a likelihood value. In Fig. 1, LVs are label at the center of each cell. Note, each cell in the active window should have a likelihood value. However, for illustrative purpose, only the 4×4 cells around robot are labeled with likelihood values. Each active cell generates a virtual attractive force, which is proportional to likelihood value and inversely proportion to the distance between the cell and the center of the vehicle. The summation of all the attractive forces, $\mathbf{F}$, is in the direction of 120 degree. This is the direction that will maximize the likelihood of locating the chemical source.

Perhaps the best-known and most often-cited problem with APF is the problem of local minima or trap situations [19]. When a local minimum appears the robot is blocked and it can not continue with the exploration (e.g., inside a U-shaped obstacle). Local minima can be created by a variety of different obstacle configurations, and different types of traps can be distinguished. In our applications, since the chemical plume is dynamically changing over time and space, it will not create trap situations for the robot. Even if trap-situations do happen, it can be resolved by heuristic or global recovery.

III. Examples

This section presents examples of the application of the algorithms that are contained in the body of this paper. In both examples, the search region is a rectangle defined by $x \in [0, 100]m$ and $y \in [-50, 50]m$. The cellular subdivision of this rectangle uses $m = 100,\ n = 100$ so that $N = 10000$ cells.

Fig. 2 and Fig. 3 show the source likelihood map at two different times during the simulation. Each figure shows the coordinates of each corner in the corresponding corner. The map is computed over the entire region for each figure. The area of interest is the smaller rectangle indicated by the dashed line. The regular grid of arrows indicate the local flow velocity at the tail of the arrow at the time the plot was generated. The plume resulting from a continual release of odor, turbulent diffusion, and advection by the fluid flow is the grey scale meandering path that begins at $(x, y) = (30, 0)$. The plume simulation model is described in [12]. The flow field is defined by the simulation model

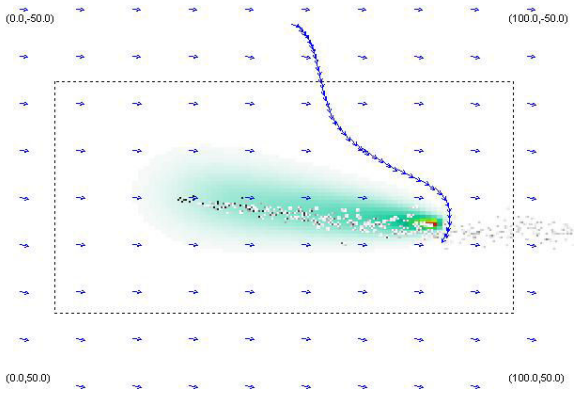

Fig. 2. Map representation of π at $t = 43s$. The trail of dark arrows moving from near the top edge down toward the plume indicates the trajectory that the vehicle followed.

and varies with both space and time as a function of time varying boundary conditions.

Fig. 2 shows a robot trajectory (The robot trajectory is indicated by the trail of blue arrows starting in $x = 50m$ and $y = -45m$ at $t = 0$. The direction of each arrow indicates the robot heading.) and a plot of source likelihood map π at time $t = 43s$. The array of colored rectangles indicates the size of source likelihood π in each cell, where darker cells have higher likelihood of containing the chemical source. The plume shape is time-varying as determined by the advection of the time-varying flow field. In this figure, the robot has just detected the plume. The source likelihood map were updated based on both detection and non-detection events. The map of π has its maximum immediately upwind of the robot location. The map of π decreases rapidly in the crosswind directions and more slowly in the upwind direction. The map spreads out as it proceeds farther upwind.

Fig. 3 shows a robot trajectory and a plot of source likelihood map π at time $t = 83s$. In this figure, the robot lost contact with the plume and tried to recover the contact with the plume near the source. After several such recover processes, the source likelihood map would accurately indicate the source location.

IV. CONCLUSIONS

This paper presents an effective olfactory-based planning and search algorithms for mobile robots operating in a turbulent flow containing a chemical plume. The derivation of the approach used a model where the chemical-filament movement in the flow is a random walk superimposed on the downflow advection. Then, based on artificial potential field methods, the robot would optimize a desired robot trajectory to navigate in the odor plume and locate the odor source location. The algorithms presented herein incorporate ideas from physics and engineering that more fully utilized the available sensor and computational resources to achieve better performance than strategies based solely on biologically inspired approaches.

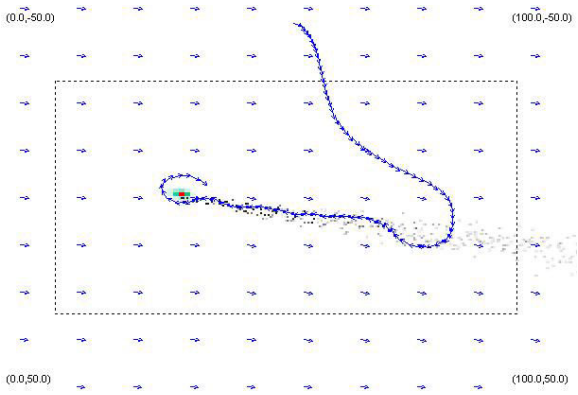

Fig. 3. Map representation of π at $t = 83s$. The trail of dark arrows moving from near the top edge down toward the plume indicates the trajectory that the vehicle followed.

V. FUTURE WORKS

Currently the algorithms are only evaluated using software simulations. However software simulations do not always show the actual real-world behavior of a system. Future work is still necessary to validate the algorithms performance in the natural environment on actual mobile robots. The first test will be a small indoor robot; if that succeeds, then it will be followed by a larger outdoor robot.

Olfactory navigation without obstacle avoidance, however, provides only limited capabilities to the autonomous vehicles in a real-world mission. For an autonomous vehicle to succeed at advanced maneuvers, a solid baseline of obstacle avoidance is mandatory. Since the APF method is based on a simple and powerful physical principle, it has an embedded obstacle avoidance capability. Besides the source likelihood map generates attractive forces, each obstacle exerts a repulsive force. Obstacles are either a priori known, (and therefore the repulsive force may be computed off-line) or on-line detected by the on-board sensors (and therefore the repulsive force is on-line evaluated). Once the on vehicle test of the olfactory based algorithms has been sufficiently demonstrated, then more advanced obstacle avoidance behaviors could be added. However, the presence of obstacles may block the air flow, generate more turbulence, and change the distribution of chemical in the environment. Therefore, the mapping algorithms presented in this paper may need to be changed significantly.

REFERENCES

[1] J. R. Andrews and N. Hogan. *Control of Manufacturing Processes and Robotic Systems*, chapter Impedance Control as a Framework for Implementing Obstacle Avoidance in a Manipulator, pages 243–251. Boston, 1983.

[2] D. E Aylor. *Perspectives in Forest Entomology*, chapter Estimating peak concentrations of pheromones in the forest, pages 177–188. Academic Press, 1976.

[3] E. Balkovsky and B. I. Shraiman. Olfactory search at high reynold number. In *Proc. Nat. Acad. Sci.*, volume 99, pages 12583–12588, 2002.

[4] J. H. Belanger and M. A. Willis. Adaptive control of odor-guided location: Behavioral flexibility as an antidote to environmental unpredictability. *Adaptive Behavior*, 4:217–253, 1998.

[5] J. H. Belanger and M. A. Willis. Biologically-inspired search algorithms for locating unseen odor sources. In *Proceedings of the 1998 IEEE ISIS/CIRA/ISAS Joint Conference on the Science and Technology of Intelligent Systems*, pages 265–270, Gaithersberg, USA, 1998.

[6] H. C. Berg. Bacterial microprocessing. In *Cold Springs Harbor Symp. Quant. Biol.*, volume 55, pages 539–545, 1990.

[7] H. C. Berg and D. A. Brown. Chemotaxis in escherichia coli analysed by three-dimensional tracking. *Nature*, 239:500504, 1972.

[8] H.C. Berg. *Random Walks in Biology*. Princeton University Press, 1993.

[9] Edwin A. Cowen and Keith B. Ward. Chemical plume tracing. *Environmental Fluid Mechanics*, 2:1–7, June 2002.

[10] D. B. Dusenbery. *Sensory Ecology: How Organisms Acquire and Respond to Information*. WH Freeman and Co, New York, 1992.

[11] J. S. Elkinton, R. T. Cardé, and C. J. Mason. Evaluation of time-average dospersion models for estimating pheromone concentration in a deciduous forest. *Journal of Chemical Ecology*, 10:1081–1108, 1984.

[12] J. A. Farrell, J. Murlis, X. Long, W. Li, and R. Cardè. Filament-based atmospheric dispersion model to achieve short time-scale structure of odor plumes. *Environmental Fluid Mechanics*, 2:143–169, 2002.

[13] F. W. Grasso. Invertebrate-inspired sensory-motor systems and autonomous, olfactory-guided exploration. *Biological Bulletin*, 200:160–168, 2001.

[14] C. D. Jones. On the structure of instantaneous plumes in the atmosphere. *Journal of Hazardous Materials*, 7:87–112, 1983.

[15] Oussama Khatib. Real-time obstacle avoidance for manipulators and mobile robots. *The International Journal of Robotics Research*, 5(1):90–98, 1986.

[16] W. Li, J. Farrell, S. Pang, and R. Arrieta. Moth behavior based subsumption architecture for chemical plume tracing on a remus autonomous underwater vehicle. *IEEE Transactions on Robotics and Automation*, 22(2):292–307, 2006.

[17] W. Li, J. A. Farrell, and R. T. Cardé. Tracking of fluid-advected odor plumes: Strategies inspired by insect orientation to pheromone. *Adaptive Behavior*, 9:143–170, 2001.

[18] C. Lytridis, E. E. Kadar, and G. S. Virk. A systematic approach to the problem of odour source localisation. *Autonomous Robots*, 20(3):261–276, June 2006.

[19] M.H. Mabrouk and C.R. McInnesa. Solving the potential field local minimum problem using internal agent states. *Robotics and Autonomous Systems*, 56(12):1050–1060, 2008.

[20] D. Martinez. Mathematical physics: On the right scent. *Nature*, 445:371–372, Jan. 2007.

[21] H. P. Moravec and A. Elfes. High resolution maps from wide angle sonar. In *IEEE Conference on Robotics and Automation*, pages 116–121, Washington D.C., 1985.

[22] J. Murlis, J. S. Elkinton, and R. T. Cardé. Odor plumes and how insects use them. *Annual. Review of Entomology*, 37:505–532, 1992.

[23] J. Murlis and C. D. Jones. ine scales structure of odor plumes in relation to insect orientation to distant pheromone and other attractant sources. *Physiological Entomology*, 6:71–86, 1981.

[24] K. R. Mylne. Concentration fluctuation measurements in a plume dispersing in a stable surface layer. *Boundary-Layer Meteorology*, 60:15–48, 1992.

[25] W. Naeema1, R. Suttona, and J. Chudley. Chemical plume tracing and odour source localisation by autonomous vehicles. *Journal of Navigation*, 60:173–190, 2007.

[26] S. Pang and J. Farrell. Chemical plume source localization. *IEEE Transactions on System, Man, and Cybernetics - Part B*, 36(5):1068–1080, 2006.

[27] B. I. Shraiman and E. D. Siggia. Scalar turbulence. *Nature*, 405(8):639–646, 2000.

[28] D. Spears, D. Zarzhitsky, and D. Thayer. Multi-robot chemical plume tracing. In *Proceedings of the 2005 International Workshop on Multi-Robot Systems*, pages 211–222, 2005.

[29] O. G. Sutton. The problem of diffusion in the lower atmosphere. *uart. J. Roy. Meteorol. Soc.*, 73:257–281, 1947.

[30] O. G. Sutton. *Micrometeorology*. McGraw-Hill, New York, 1953.

[31] Massimo Vergassola, Emmanuel Villermaux, and Boris I. Shraiman. infotaxis as a strategy for searching without gradients. *Nature*, 445:406–409, Jan 2007.

[32] D. Zarzhitsky, D. Spears, D. Thayer, and W. Spears. Agent-based chemical plume tracing using fluid dynamics. *Lecture Notes in Artificial Intelligence*, 3228:146–160, 2004.